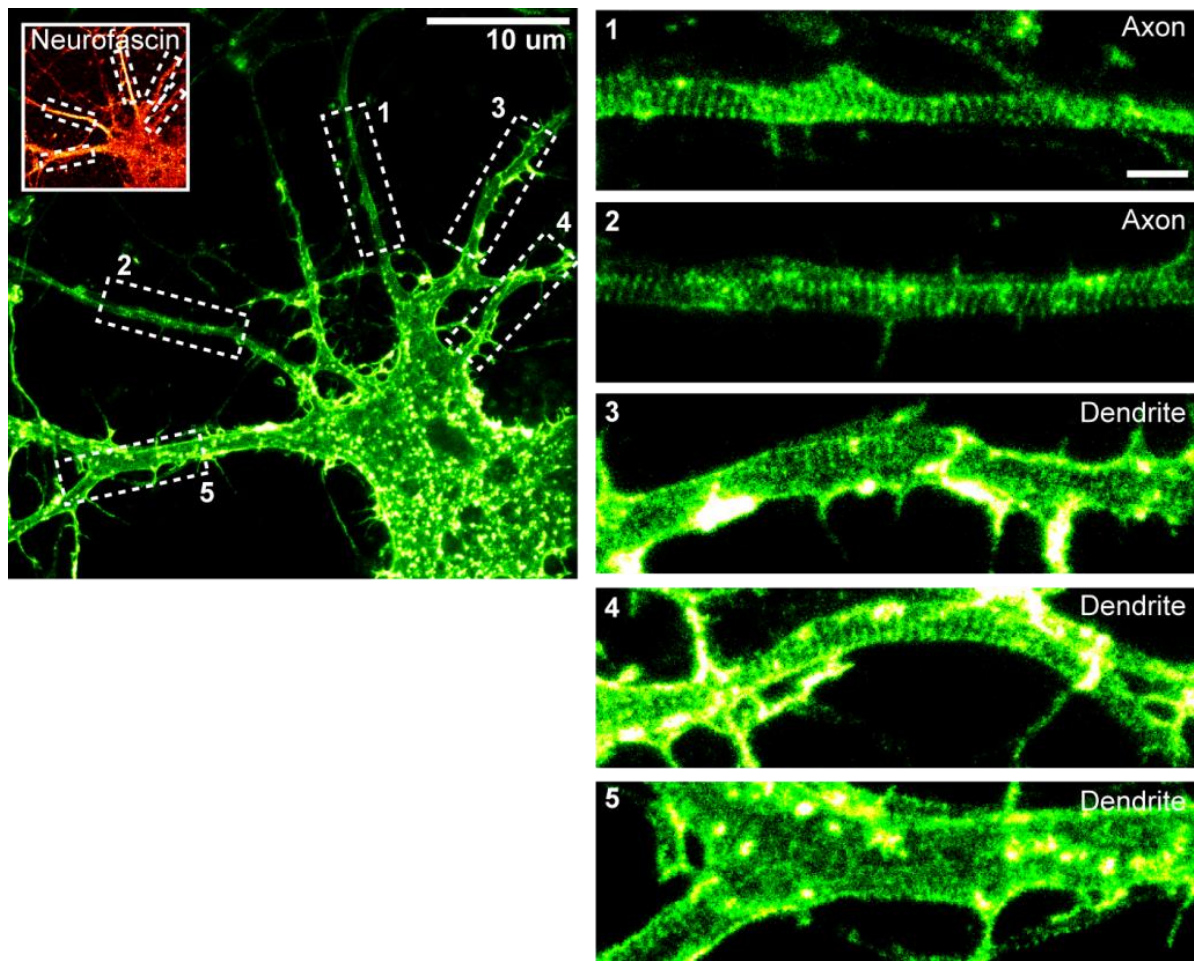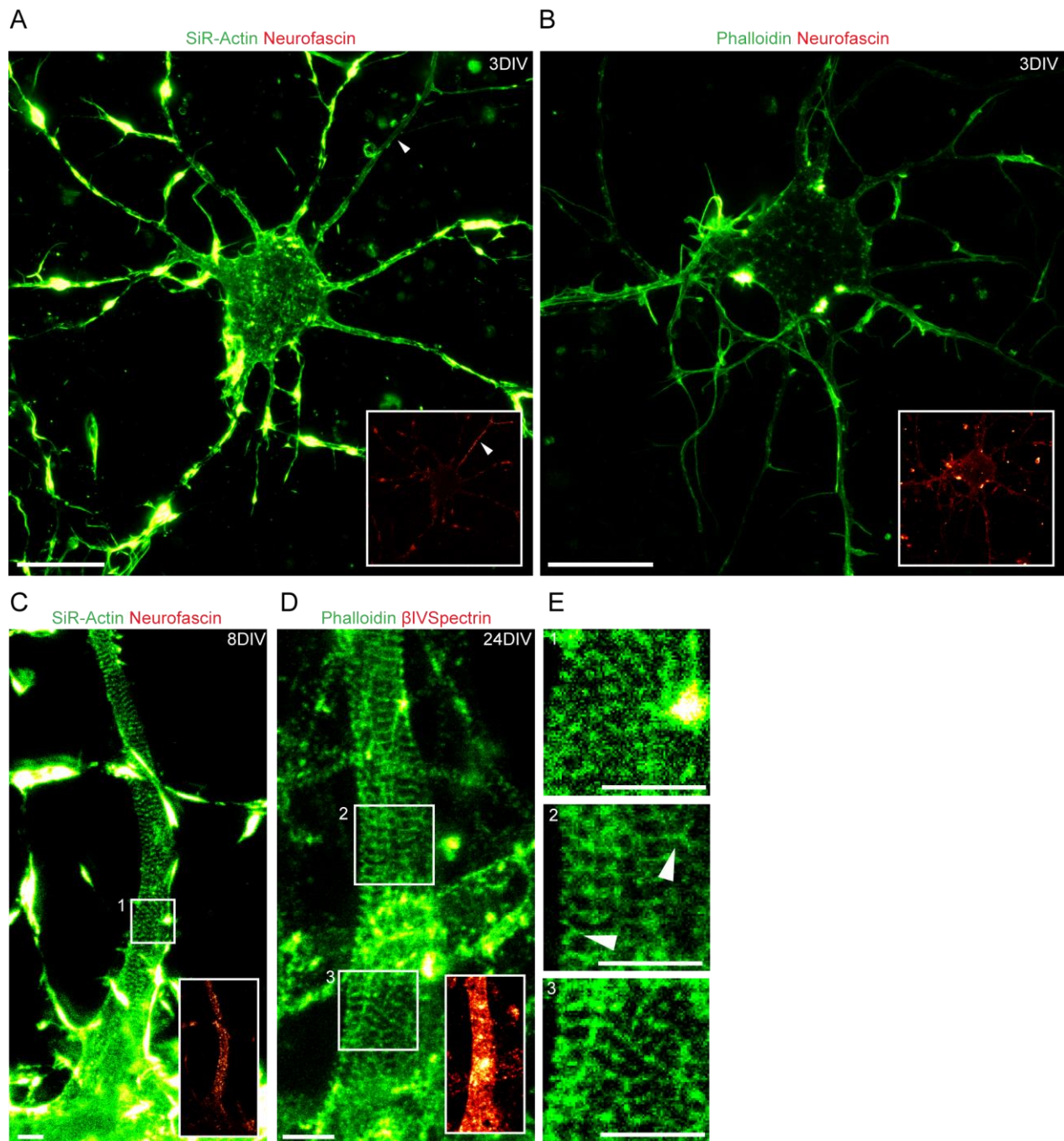**Cell Reports**

Supplemental Information

STED Nanoscopy Reveals the Ubiquity of Subcortical Cytoskeleton Periodicity in Living Neurons

Elisa D'Este, Dirk Kamin, Fabian Göttfert, Ahmed El-Hady, and Stefan W. Hell
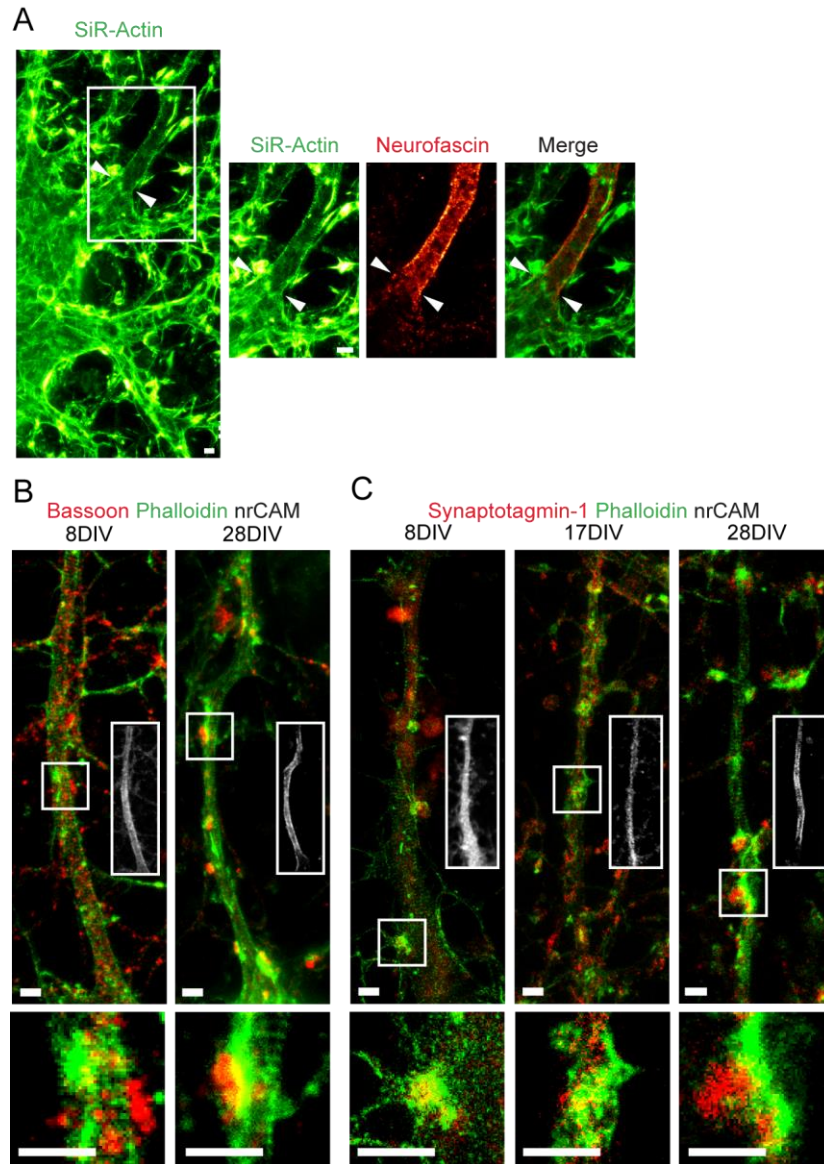
Supplemental Figures

Figure S1: Phalloidin staining confirms the presence of a periodic structure of actin also in neurofascin negative neurites. Related to Figure 1. STED image of a fixed neuron at 8 DIV in which actin stripes are present also in dendrites. Neurons were stained with phalloidin-STAR635 and neurofascin (inset) to highlight the axon. Note that the neuron exhibits two axons (strong signal, inset). On the right, closeups of the boxed regions are shown. Boxes 1 and 2 correspond to neurites positive for neurofascin (i.e. axons), while boxes 3-5 correspond to neurites that are negative for neurofascin (dendrites). Scale bars 1μm. All pictures depict raw data.

Figure S2: Features of cortical actin organization. Related to Figure 2. (A,B) Features of cortical actin organization. **(A)** STED image of a living hippocampal neuron stained with SiR-Actin (3 DIV). Inset shows the respective neurofascin staining. Arrowhead indicates a neurite enriched in neurofascin and in which an actin periodic pattern is visible (close up is shown in **Figure 2A**). **(B)** STED image of a phalloidin-stained neuron (fixed, 3 DIV). Inset shows the

respective neurofascin staining. Scale bars 10 µm. **(C, D, E)** Actin can form a more complex actin lattice. **(C)** STED image of a living hippocampal neuron stained with SiR-Actin (8 DIV). Inset shows the respective neurofascin staining to mark the AIS. SiR-Actin reveals an actin structure more complex than simple actin rings (respective box 1 in **(E)**). **(D)** STED image of a phalloidin-stained neuron (fixed, 24 DIV). Inset shows the respective βIVspectrin staining to mark the AIS. The white boxes indicate the respective enlarged regions in **(E)** (boxes 2 and 3). Like SiR-Actin, phalloidin additionally clearly reveals examples of branched filaments (arrowheads, box 2). All scale bars 1 µm. All images depict raw STED data.

Figure S3: Features of cytosolic actin organization. Related to figure 4. (A) The cytosolic actin organizational border. STED image of both the axon (neurofascin-positive) and some dendrites of a living neuron (17 DIV). The white box indicates the respective magnified views to the right. Arrowheads indicate where neurofascin (and hence the AIS) begins. Note the difference in cytosolic actin organization between the axon and the dendrite at the bottom right of the magnified images. **(B,C)** Actin accumulates at synaptic boutons during development. **(B)** Co-localization of actin patches (phalloidin staining, green) with bassoon (red) in neurons at 8 and 28 DIV (see **Figure 4C** for 17 DIV). Axon was identified by staining NrCAM (insets, white).

(C) Same as **(B)** but with synaptotagmin-1, at 8, 17 and 28 DIV. Note that anti-synaptotagmin-1 antibody was directly coupled to Atto647N dye. Actin patches become more prominent as bassoon and synaptotagmin-1 accumulate at synaptic boutons. Scale bars 1μm. All images are raw data.

Supplemental Experimental Procedures

Primary hippocampal neuron culture preparation

Cultures of hippocampal neurons were prepared from Wistar rats of mixed sex at postnatal day P0–P1 in accordance with the regulations of the German Animal Welfare Act and under the approval of the local veterinary service. Cells were plated on coverslips coated with 100 µg/ml polyornithine (Sigma-Aldrich, cat. P3655) and 1 µg/ml laminin (BD Bioscience, cat. 354232). Neuronal cultures were maintained in Neurobasal medium (Gibco, cat. 21103049) supplemented with 2% B27 serum-free supplement (Gibco, cat. 17504044), 2 mM L-glutamine (Gibco, cat. 25030) and pen/strep (100 units/ml and 100 µg/ml, respectively, BiochromAG, cat. A2213). On the day after plating, 5 µM cytosine β-D-arabinofuranoside (Sigma, cat. C1768) was added to the cultures. Medium was replaced once per week.

Live-cell staining

Live-cell staining of actin was achieved by adding the SiR-Actin probe from a 1 mM DMSO stock solution to the growth medium at a final concentration of 2 µM. Cells were incubated for 1 h in a humidified 5% CO_2 incubator at 37°C. SiR-Actin was a kind gift of Kai Johnsson and Grazvydas Lukinavicius (both at EPFL, Lausanne, Switzerland) and is now commercially available (Spirochrome, cat. SC001).

The axon initial segment was stained for 5 min at RT with an anti–pan-neurofascin antibody (UC Davis/NIH NeuroMab Facility, cat. 75-172, 10 µg/mL), recognizing the extracellular domain of the protein, diluted in artificial cerebrospinal fluid (ACSF buffer). After three fast washes with ACSF, cells were incubated for 30 s with STAR580 (Abberior, cat. 1-0101-005-2)-labeled sheep anti-mouse secondary antibody (Dianova, cat. 515-005-003). After washing, cells were imaged in ACSF buffer at RT.

Immunostaining

Cells were washed with PBS and fixed in 4% PFA in PBS (pH 7.4) for 20 min at RT, quenched with NH_4Cl and glycine (100 mM each) for 5 min and permeabilized with 0.1% Triton X-100 for another 5 min. Both primary and secondary antibody and phalloidin incubations were performed in PBS for 1 h at RT or overnight at 4°C. Samples were mounted in Mowiol supplemented with DABCO. Incubations with phalloidin and anti-synaptotagmin-1-Atto647N antibody were performed together with the secondary antibodies.

Sciatic nerve preparation

Sciatic nerves were extracted from 3-4 months old C57BL/6 mice (both sexes), teased and frozen at -20°C on a coverslide. Samples were then fixed in ice cold methanol (-20°C) on ice for 10 min, permeabilized with 0.5% Triton X-100 in PBS for 45 min and re-equilibrated in PBS containing 0.05% Triton X-100. Both primary and secondary antibody incubations were performed for 1 h at RT in PBS supplemented with 0.05% Triton X-100. After each step, samples were rinsed 3 times for 10 min with 0.05% Triton X-100.

Samples were afterwards embedded in melamine as described before (Punge et al., 2008), following a controlled temperature regime (24 h at RT, 24 h at 40°C and 48 h at 60°C). After complete polymerization, sections of 250-500 nm thickness were cut using an ultramicrotome (EM UC6, Leica Microsystems, Wetzlar, Germany).

STED microscope

The images were obtained with a STED nanoscope described previously (Göttfert et al., 2013). Excitation of the fluorophores was performed with two pulsed diode lasers emitting ≈70 ps pulses, one at 595 nm, the other at 640 nm (both from PicoQuant, Berlin, Germany). To increase spatial resolution beyond the diffraction limit, we manipulated the beam of a pulsed, 775-nm-wavelength fiber laser (IPG Photonics) so that the focal intensity distribution exhibited a

central intensity of ~0, while the increasing intensity switches off the fluorescence ability of fluorophores surrounding the very focus center by stimulated emission. The result is a subdiffraction-sized probing area for confocal laser scanning STED nanoscopy. Using pulse energies of 3 nJ, we achieved resolutions of 30-40 nm. The excitation and STED beams were co-aligned and coupled into a 1.4 numerical aperture oil immersion lens (NA 1.4 HCX PL APO, 100x, Leica Microsystems). Sample fluorescence was collected by the same lens, spectrally separated and filtered into two ranges: 600-640 nm and 660-720 nm. The images were acquired by scanning the sample with a piezo stage (Mad City Labs) and detecting the fluorescence with an avalanche photodiode (Micro Photon Devices). A conventional confocal (i.e., diffraction-limited resolution) channel with 470 nm excitation and 500-550 nm detection wavelengths was implemented to additionally image Alexa488. The overlay of the STED and confocal channels was adjusted and verified on 100 nm TetraSpeck fluorescent beads (Life Technologies).

Processing and visualization of acquired images.

All acquired or reconstructed images were processed and visualized using ImSpector software (Max-Planck Innovation) and ImageJ (imagej.nih.gov/ij/). For visualization of the images, the "fire" and "delta" lookup tables (LUTs) of ImSpector were used. Brightness and contrast were linearly adjusted for the entire images. Line profiles were measured with ImageJ software along a 3-5 pixel wide line (for cultured neurons) or a 5-15 pixel wide line (for nodes of Ranvier). Interpeak distances were determined using the multi-peak fitting function in OriginPro8.5.